Strain: Observations of the Vertical Gradient of Isopycnal Vertical Displacement

ROBERT PINKEL, JEFFREY SHERMAN, JEROME SMITH AND STEVEN ANDERSON

Marine Physical Laboratory of the Scripps Institution of Oceanography, University of California, San Diego, La Jolla, California

(Manuscript received 3 October 1989, in final form 15 October 1990)

ABSTRACT

In this work a profiling CTD, operated from the research platform *FLIP*, is used to monitor the fine-scale density field as a function of both depth and time. A sequence of 10 000 CTD profiles from the surface to 560 m is examined. The data were obtained off the Southern California coast in the 1986 PATCHEX experiment. The vertical separation between successive isopycnal surfaces is tracked. The separation is related to the vertical derivative of vertical displacement, and is here referred to as the strain. The purpose of this work is to present a simple picture of the fine scale strain field as it evolves in time as well as depth.

When viewed in isopycnal following coordinates, the qualitative nature of the strain field depends on the characteristic vertical scale over which it is estimated. The "20 m strain" field has a wavelike character, dominated by inertial and semidiurnal tidal motion. Wavelike fluctuations are seen in the 20 m strain field even at subinertial frequencies. This suggests that nonlinear processes are significant even at these relatively large vertical scales. The "2 m strain" more closely resembles the classic picture of fine structure. Lenses of low density gradient fluid are separated by sheets of higher gradient water. The lenses are seen to persist up to eight hours. They can propagate with respect to the density field over tens of meters. The low gradient regions evolve into regions of high gradient and visa versa. The probability density function (PDF) of isopycnal separation is Gaussian for isopycnal pairs of large ($\sim$20 m) mean separation. As mean separation distance is decreased, the skewness of the distribution increases.

Since all scalar fields in the sea are strained by the same velocity field, fluctuations in the fine-scale vertical gradients of a variety of quantities are correlated. Averages of the products of fine scale gradients can differ significantly from products of the averages.

1. Introduction

In recent decades considerable progress has been made at determining the space–time scales of the internal wavefield (Garrett and Munk 1972, 1975, 1979; Munk 1981). Emphasis has generally been placed on the energy containing features of the field, such as near inertial waves or the baroclinic tide. Fine-scale (1–50 m in the vertical) aspects of the motion field are known primarily through vertical profiling observations. Candidate vertical wavenumber spectra of shear (Gargett et al. 1981) and strain/temperature gradient (Gregg 1977) are now generally accepted. However, little is known about the appropriate lateral and temporal scales associated with the observed fluctuations of shear or strain in depth.

As a step in this direction, we present observations of the fine-scale strain field in both depth and time. The data are collected using a repeated profiling CTD system (Pinkel 1975) operated from the research platform *FLIP*. A set of 10 000 profiles from the surface to 560 m is the basis for this study. The data were obtained as part of an overall program to observe both shear and strain fields simultaneously (Sherman 1989; Sherman and Pinkel 1991). The strain measurement is in some sense the most satisfying, in that a broad range of vertical scales is covered and the fine scale signal is easily seen above measurement noise. Importantly, the time evolution of the strain field can be conveniently observed in either an Eulerian (fixed depth) frame or in isopycnal following coordinates. The views obtained in these two frames are quite different (Sherman and Pinkel 1991). The difference is due to the vertical advection of the fine scale field by the internal wavefield itself. The vertical advection effect has been considered a source of "contamination" of Eulerian measurements and has been studied from that point of view (Phillips 1971; Garrett and Munk 1971; McKean 1974). In an isopycnal following frame, the so-called "fine-structure contamination" problem is avoided. Time evolution of the observed field will depend on the vertical rate of strain, $\partial w/\partial z$, rather than vertical velocity itself.

Operating in an isopycnal following frame is not without an attendant set of subtleties. Isopycnal fol-

Corresponding author address: Dr. Robert Pinkel, Marine Physical Lab. of the Scripps Institution of Oceanography, University of California, San Diego, La Jolla, CA 92093.

lowing coordinates are neither Eulerian nor Lagrangian. To illustrate the nature of situations which can occur when in isopycnal following coordinates, consider the process of time averaging. In Fig. 1, 20-day averages of density gradient are plotted. The gradients are calculated at a set of 470 fixed depths, (90–560 m) and at 470 variable depths, as well. The variable depths represent the instantaneous positions of isopycnal whose *mean* depths correspond to the respective fixed depths. It is seen that averages of the density gradient are approximately 50% greater in the isopycnal following (semi-Lagrangian) frame than in the Eulerian frame. This rather odd result is an inherent property of observing in isopycnal following coordinates. It results from the non-Gaussian nature of the fine scale field.

The purpose of this paper is to describe qualitatively the depth–time evolution of the strain field. The changing nature of the field will be noted as the characteristic vertical scale of the observation is reduced from internal wave (~20 m) to extremely fine (~2 m) scales. Strain statistics become progressively less Gaussian with decreasing vertical scale. Depth (density)–time statistics of the occurrence of extremely high and low strain events are presented. An extended discussion, again primarily qualitative, suggests why this non-Gaussianity is observed and lists some general oceanographic implications.

The tone of the discussion is similar to that of the pioneering statistical studies of Desaubies and Gregg (1981) and Desaubies and Smith (1982), although influenced by present ability to work in isopycnal following coordinates. The discussion is based on the assumption of the existence of some mean, monotonic density profile, which is equivalently expressed as $\bar{\rho}(z)$ or $Z(\rho)$. The profile is distorted under the straining influence of the motion field. The distortion is seen through the vertical displacement of various isopycnals

$$\eta(t, \rho) = z(t, \rho) - Z(\rho). \quad (1)$$

Using this notation one can describe a depth–time field of isopycnal depth difference as

$$\Delta z(t, \bar{z}, \overline{\Delta z}) = z(t, \rho_1) - z(t, \rho_2). \quad (2)$$

Here $\bar{z} \equiv (Z(\rho_1) + Z(\rho_2))/2$ is the mean depth of the isopycnal pair and $\overline{\Delta z} \equiv (Z(\rho_1) - Z(\rho_2))$ is the mean separation. Protagonists in the present study are the normalized depth difference

$$\gamma(t, \bar{z}, \overline{\Delta z}) = \Delta z/\overline{\Delta z}, \quad (3)$$

a positive quantity (as isopycnals cannot cross), and the finite difference strain

$$\hat{\gamma}(t, \bar{z}, \overline{\Delta z}) = \gamma - 1 = (\Delta z - \overline{\Delta z})/\overline{\Delta z}. \quad (4)$$

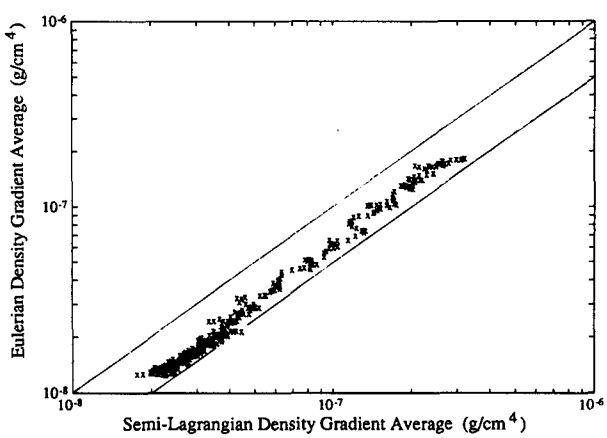

FIG. 1. Averages of density gradient at fixed depth $\bar{z}$, as a function of the density gradient averaged along the corresponding fixed density, ρ, where $\rho = \bar{\rho}(\bar{z})$. Averages are formed from 9600 profiles obtained over a 20 day period. Eulerian gradients are formed from 40 cm first differences of the density profile, centered at fixed depths. The semi-Lagrangian gradients are estimated from 40 cm differences which span the isopycnal whose mean depth is that of the corresponding Eulerian estimate. Data from 90 to 560 m are included in the plot. The semi-Lagrangian average exceeds the Eulerian average by a factor of approximately 1.7, at 400–500 m, to 1.4 in the high gradient region of the water column.

2. Experiment description

The data are derived from density profiles obtained from a profiling CTD system on the Research Platform *FLIP*. Ten thousand profiles were collected from the surface to 560 m in the 1986 PATCHEX Experiment. The PATCHEX site was 34°N, 127°W, about 500 km west of Pt. Conception, California. Water depth is 4 km. *FLIP* was placed in a two-point taut moor, restricting lateral motion to an area of several hundred meters square.

Seabird Instruments model SBE-9 CTD systems were used, following modification for high speed operation. The modifications included the construction of an open cylindrical frame to protect and support the instrument and the addition of a weighted (25 kg lead shot) nose piece to increase the fall rate. A static pressure port was interfaced to the Digiquartz pressure sensor, to reduce the magnitude of turbulent pressure fluctuations associated with the high fall rate.

In PATCHEX, a pair of instruments covered the depth ranges 0–300 m and 260–560 m. The CTDs were cycled every three minutes, corresponding to a drop rate of 3.8 m s^{-1}. The Nyquist frequency, 10 cph, was not sufficient to prevent aliasing of internal wave motions in the upper thermocline (80–150 m). The aliasing of low mode internal wave motions is the dominant high frequency noise in these measurements.

The instruments are sampled at 12 Hz, corresponding to a sampling distance of 32 cm. Given the high fall rate, it is not necessary to pump the conductivity cell to achieve reasonable spatial resolution. The phase

and amplitude response of the conductivity sensor is matched to that of the temperature sensor. $T - C$ gradient cross spectra, estimated from data in nearly isohaline regions of the water column, are used to determine the relative response of the instruments. Following the response matching, the outputs of both sensors are lowpass filtered with a 2 m cutoff, to assure uniform high wavenumber response. (Sherman 1989). Potential temperature, salinity and potential density profiles are obtained from the response corrected CTD information. Cruise-averaged profiles are computed. A set of reference densities, whose mean depths are separated by 1 m, is then chosen. The encounter depth of each of these reference densities (isopycnals) is computed for each profile using linear interpolation.

3. Observations

In this section the isopycnal information is first used to describe the large scale vertical displacement field. Subsequent plots display strain calculated on progressively finer depth and time scales. The objective here is to contrast qualitatively the nature of the motions at the various scales.

In Fig. 2 we see the isopycnal displacement field during PATCHEX.

Clearly apparent in the motion field is the semidiurnal baroclinic tide. This has vertical wavelength long compared to the 400 m observation depth and vertical displacements as great as 30 m, crest-to-trough. Some evidence of a spring–neap fluctuation in amplitude is seen, particularly at depth.

The fine vertical scale motions of interest in this study are obscured by the tide and the other higher frequency constituents of the wavefield, which are highly coherent with depth. To view the smaller scale field, it is convenient to form plots of isopycnal depth difference, $\Delta z(t)$. These can be plotted against either the instantaneous mean depth of the isopycnal pair or against the cruise averaged mean depth of the pair, $\bar{z}$. In the latter case the time evolution of the field is seen in a "semi-Lagrangian" frame, with $\bar{z}$ effectively serving as a label for the isopycnal pair. In Fig. 3, the depth–time series of 20 m strain, $\Delta z(t, \bar{z}, 20)$, is plotted. This is a record of the instantaneous difference in depth between an isopycnal whose mean depth is 10 m above the depth signified in the ordinate and one whose mean depth is 10 m below. The two hour smoothing nearly obscures the period on day 4 when no data were taken. The dominant signals apparent in the 20 m strain are associated with both inertial waves and semidiurnal motions. The vertical coherence of the tidal strain signal is greatly reduced when compared to the displacement signal. This is to be expected, as the strain is effectively the derivative of displacement with respect to depth. The vertical wavenumber dependence of the strain spectrum is "less red" than that of displacement by the factor k_z^2. While the strain field has a lumpy and irregular aspect in general, there are periods where both upward and downward phase propagation are seen.

It is perhaps surprising to see a strong inertial signal

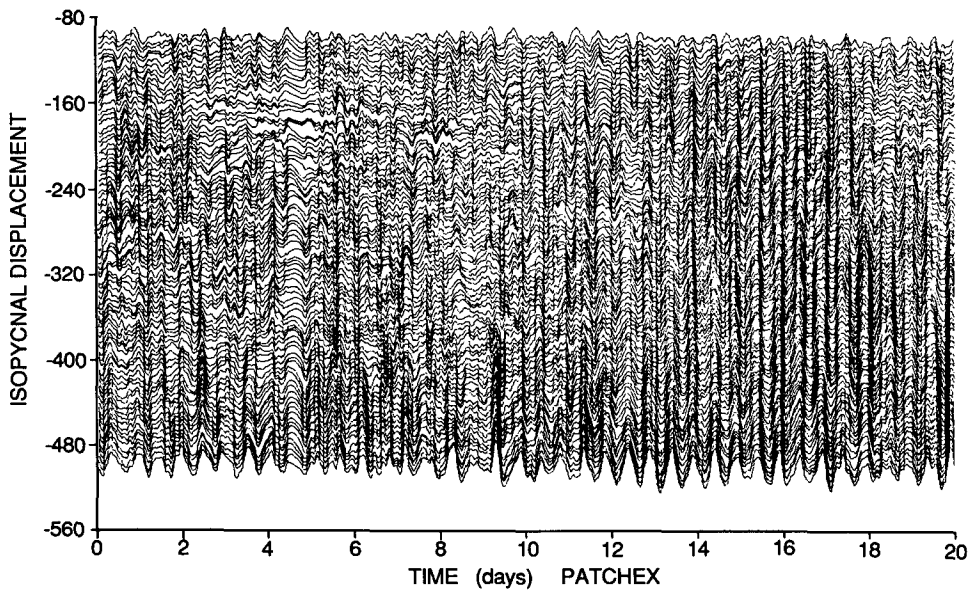

FIG. 2. The vertical displacement field observed in the 1986 experiment, PATCHEX. One hundred isopycnal surfaces, each separated by 5 m in the mean, are tracked. The record starts at noon local time, 6 October and is smoothed by a two hour running mean filter. The filtering partially obscures a 6 hour period (days 4.2–4.5) when data were not collected.

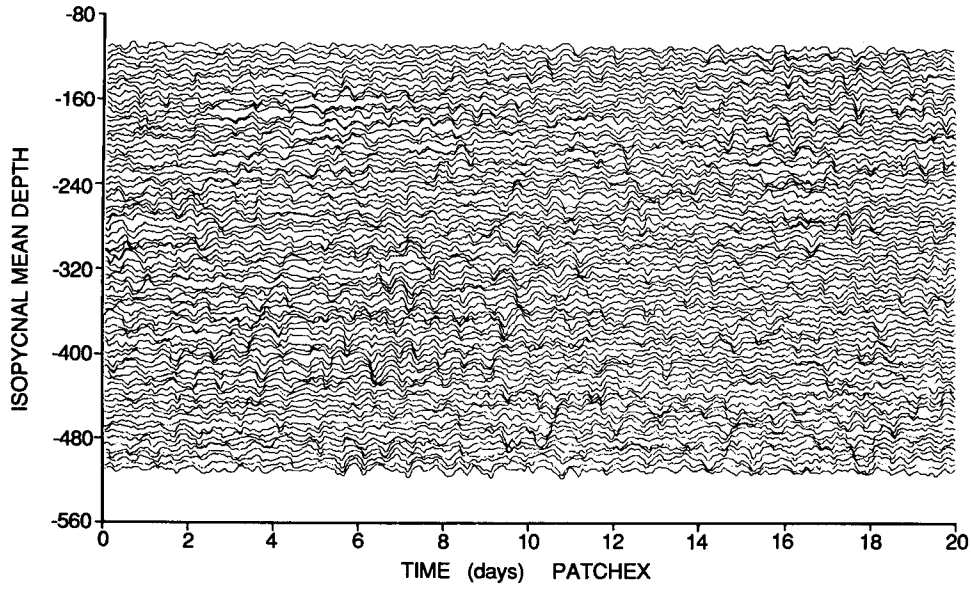

FIG. 3. Twenty meter isopycnal strain or depth-difference time series. Vertical excursions of these lines are proportional to the separation between isopycnals whose mean separation is 20 m. The record starts at noon local time, 6 Oct 1986, and is smoothed by a two-hour running mean filter. Successive strain series are offset in depth, in proportion to the mean depth of the isopycnal pair. Isopycnal following removes the effect of the gross vertical advection of the internal wavefield.

in the strain field. Linear inertial motions are not expected to produce a vertical displacement signature. Nevertheless, the signal is present. In the 1983 experiment, MILDEX, power spectra of strain (Pinkel et al. 1987, Fig. 10f) also reveal weak inertial as well as tidal peaks. When contrasted with other Southern California observations (Pinkel 1984) the near inertial field in PATCHEX is relatively weak. It is likely that the near inertial signal is a ubiquitous feature of the strain field.

It has been suggested (Holloway 1983; Muller 1984) that much of the strain signal might not be due to internal waves, but rather to the small-scale analog of two dimensional quasi-geostrophic turbulence. An apparently reasonable test of this hypothesis is to examine sub-inertial frequencies, where internal waves presumably do not exist. In Fig. 4, a 20 day record of isopycnal depth difference is again presented. Here the smoothing period is 24 hours, rather than the 2 h used previously. A simple running mean filter is used. Surprisingly, wavelike motions are again seen. Evidence of cross isopycnal propagation, clearly not a feature of two dimensional turbulence, is seen throughout the record.

In the discussion section below, a simple nonlinear model for isopycnal straining is introduced. A quadratic nonlinearity allows the isopycnal strain signature to appear at sum and difference frequencies (and wavenumbers) of the underlying motion field. Higher order nonlinearity enables even greater "leakage" of the strain signal out of the internal wave band. Thus the internal wavefield might be responsible for these observed sub-inertial variations in isopycnal separation.

The dominant motions in Figs. 3, 4 have vertical scales of tens of meters. Most of the strain variance occurs at far smaller scale. We can focus on the smaller scale motions by considering the depth difference between isopycnals whose mean separation is 5 m rather than 20 m.

In Fig. 5 the logarithm of 5 m isopycnal separation is plotted over a 24 hour period. The displacement of the profiles to the right in Fig. 5 corresponds to large isopycnal separation, a layer of depressed local Väisälä frequency. Displacement to the left corresponds to small isopycnal separation, a sheet of enhanced stability. The vertical profile format is a concise method for providing a large scale look at the fine scale field. Depth difference information from 400 isopycnals is incorporated in Fig. 5. Cross-isopycnal propagation of features, when it occurs, is easily detectable. The depth difference profiles themselves are skewed. Isopycnals can never be closer together than 5 m from their mean position. They can be arbitrarily far apart. By taking the logarithm of separation, the apparent asymmetry in the profiles is greatly reduced.

In this plot of 15-min averaged strain profiles, there is little evidence of the large scale semidiurnal signals which are prominent in Fig. 3. Here one sees motions which appear as isolated lumps, slowly propagating vertically across isopycnal surfaces. The maximum rate of phase propagation is of order 4 m $h^{-1} \sim 10^{-1}$ cm s^{-1} relative to the large scale field.

It is likely that horizontal advection influences the observed time evolution. Consider a linear internal wave group with characteristic vertical wavenumber 0.1 cpm and intrinsic frequency midway between the

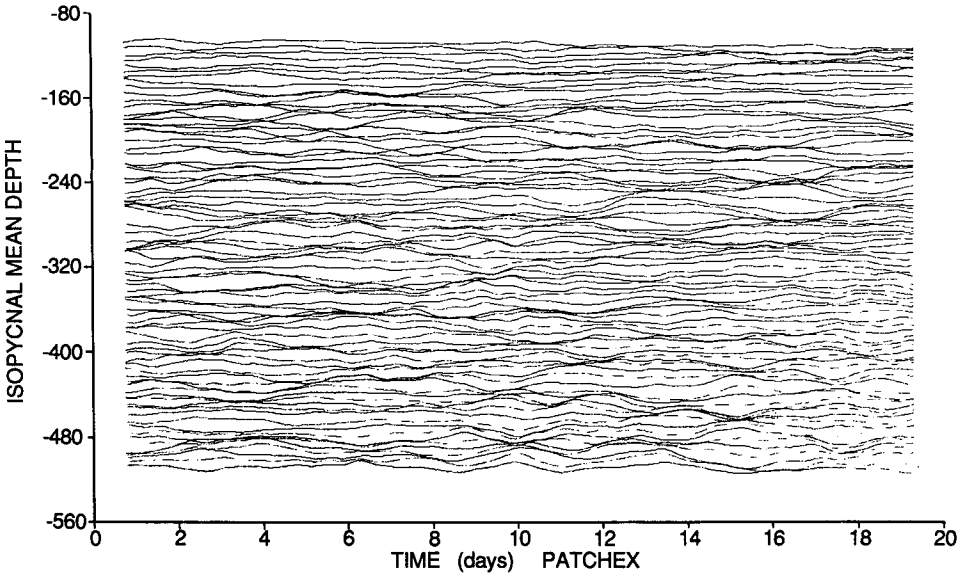

FIG. 4. Subinertial strain. Data are as in Fig. 3 except smoothed with a 24-hour running mean filter, to reveal the subinertial strain field. The vertical scale here has been exaggerated relative to that of Fig. 3 by a factor of 3.33.

inertial and Väisälä frequencies. The characteristic horizontal phase speed, c, is

$$c = \frac{\omega}{k_H} \approx \frac{N}{k_z} = 1 \text{ cm s}^{-1}. \quad (5)$$

Here, N, the local Väisälä frequency, is taken as 3.6 cph and k_H, k_z are horizontal and vertical wavenumbers, respectively. As typical horizontal advection speeds are typically larger than 1 cm s^{-1}, spatial as well as temporal variation is being observed in these figures.

In Fig. 6, the logarithm of 2 m isopycnal separation is presented. Profiles are presented every 3 minutes for a single day of the PATCHEX experiment. As in Fig. 5, layers or lenses of nearly constant density appear as

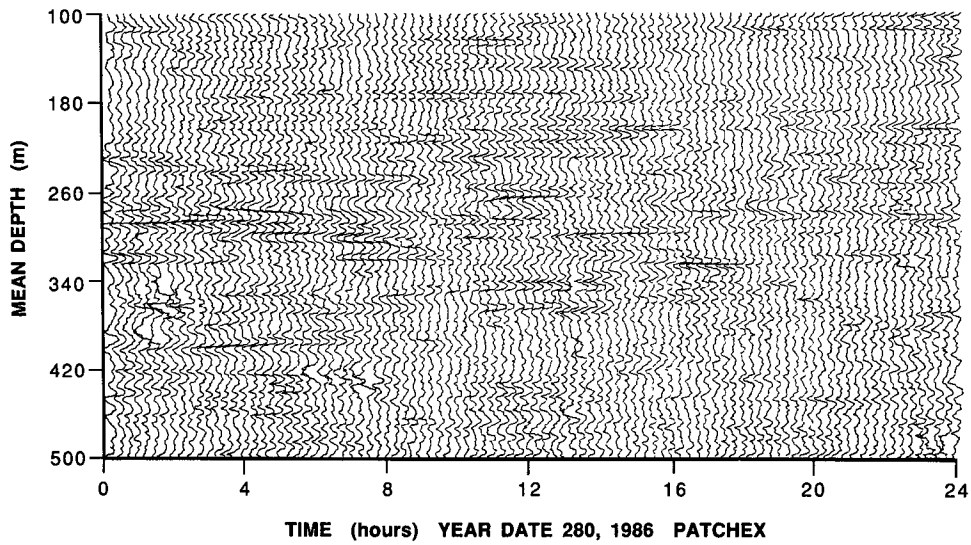

FIG. 5. Five meter strain: the logarithm of instantaneous separation between isopycnals whose mean separation is 5 m. Depth differences are averaged over 15 min prior to forming these profiles. Data are plotted as a function of isopycnal mean depth. Excursions to the right correspond to large isopycnal separations, or layers. Excursions to the left correspond to small isopycnal separation, sheets. An excursion equivalent to the mean offset between profiles corresponds to a factor of $\frac{1}{3}$, 3 departure from the mean isopycnal separation. The signal consists predominately of isolated events which persist for a fraction of a day, and propagate significantly with respect to the density field. Data are from year day 280, 1986.

fine, nearly horizontal lines. Cross isopycnal propagation of these lenses is often seen (0200 at 300 m or 0800 at 320 m, for example). The layers persist for periods up to six hours. The evolution of these layers takes place against a fine-scale background which is remarkably repeatable in detail, except in isolated depth–time regions of rapid and irregular change. The region above 200 m is typically quiescent, with the smallest details in the strain profiles repeatable over periods of an hour or more.

The regions of rapid variation (e.g., 340–380 m at 0100) stand out strongly in Fig. 6. The physical phenomenon that causes this effect is not known. It was originally suspected that problems associated with estimating density from the conductivity and temperature sensors on the CTD were responsible for the periods of irregularity. However, analogous plots using only temperature data show similar behavior. It remains to investigate the correlation of occurrence of these active patches with the horizontal velocity and shear fields measured using the Doppler sonars on *FLIP*. If patches tend to occur during periods of high horizontal velocity, the advection of small horizontal scale perturbations in the density field must be considered. If they occur during periods of low velocity, instrument wake might be responsible.

The relative abruptness of the 2 m strain tends to overshadow much of the less dramatic detail in Fig. 6. An enlarged view of the upper 160 m of the figure is replotted in Fig. 7. Here the finest scales resolvable by the CTD are seen. When viewed in isopycnal following coordinates, the profile-to-profile repeatability of the fine scale features is impressive. The apparent lifetime of the modest strain "events" is comparable to that of the extreme sheets or layers.

Note the similarity in appearance of Figs. 5 and 7. The 160 m record of 2 m strain has the same qualitative character as the 5 m strain, over a depth interval $5/2$ times greater. No ad hoc rescaling of the plots has been done to enhance their resemblance. From inspection of the raw strain profiles, one can deduce only the ratio of $\overline{\Delta z}$ to the total field of view. Neither parameter, alone, can be estimated from an "unlabeled" dataset. The tendency toward self-similar behavior in the strain field will be discussed below.

The apparent homogeneity of Figs. 5–7 with depth is also notable. Internal wave displacement and velocity fields are strongly influenced by depth variations in the Väisälä frequency. Plots of large scale fields must be appropriately "Väisälä stretched" in order to remove the refractive distortion. The Väisälä distortion of the strain field is apparently more subtle than that of displacement and velocity. The relative lack of dependence of strain on Väisälä frequency is consistent with linear internal wave theory in the WKB approximation. More sensitive tests are called for to investigate this issue in detail.

4. Strain statistics

The character of the strain field changes markedly between 20 m and 5 m vertical scale. The differences between the 5 m and 2 m strain fields are less obvious. Simple statistics can be presented to emphasize the effect of changing scale. In Fig. 8, the isopycnal depth difference variance is plotted as a function of mean vertical separation, $\overline{\Delta z}$. Patterns from four depth zones are presented. At mean separations greater than 10 m, the variance is seen to increase linearly with mean separation. This is consistent with a strain spectrum which is essentially white in vertical wavenumbers less than 0.1 cpm (Appendix). The straight lines, if extrapolated

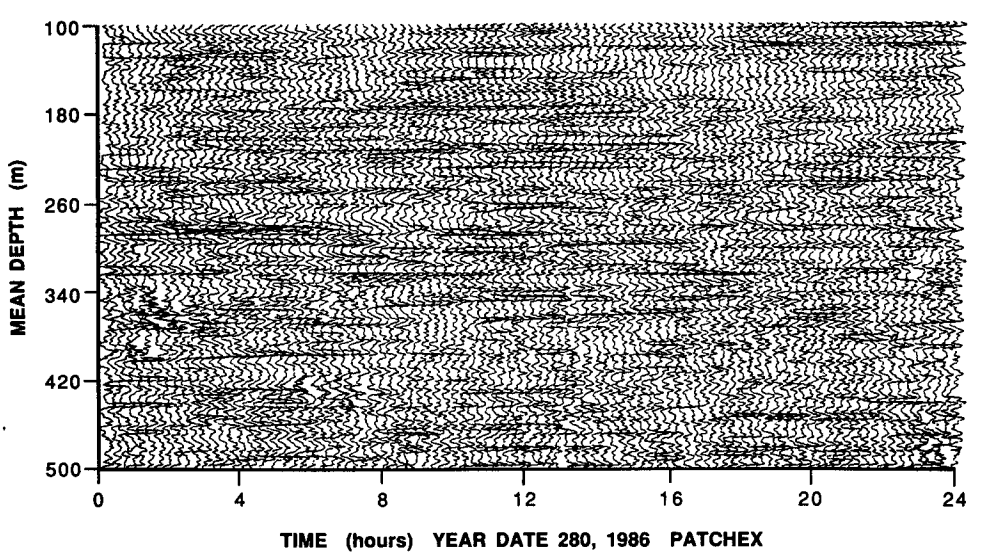

FIG. 6. The logarithm of two meter strain. Depth difference profiles are presented every 15 min. The data are from year day 280, 1986, as in Figs. 5, 7. The scaling of the abscissa is unchanged from Fig. 5.

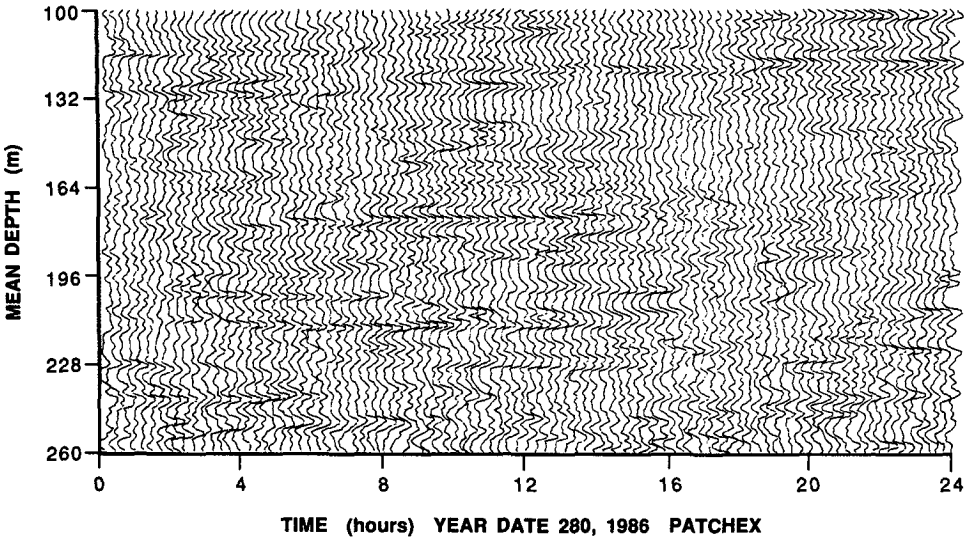

FIG. 7. The logarithm of two meter strain. An enlargement of the top 160 m of Fig. 6. The scaling of the abscissa is unchanged.

to small separation, do not indicate zero variance at zero mean separation. The actual curves indeed roll down at less than 10 m, providing a physically sensible result. The roll down is a consequence of the finite variance of the strain spectrum (Appendix).

At very large mean separations (not shown in Fig. 8), where the participating isopycnals are uncorrelated, the variance should approach a constant value, equal to twice the variance of the individual isopycnal displacements.

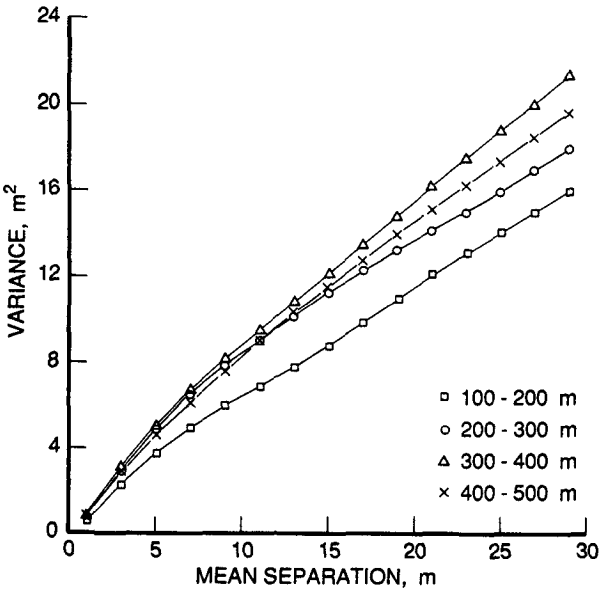

FIG. 8. The variance of isopycnal displacement difference $\langle \Delta z^2 \rangle$ as a function of mean separation Δz.

The mean separation and variance are not adequate to describe the statistics of the strain measurements. This is seen in Figs. 9, 10, and 11 where representative probability density functions of isopycnal separation are presented. The "events" recorded in these PDFs represent individual encounters of the isopycnal pairs during the first 9000 profiles of the PATCHEX experiment. The events are equally sampled in time but not necessarily in depth. Each histogram records the distribution of nearly two million observations. However, adjacent events in time are highly correlated. The profiles are repeated 20 times per hour and the correlation time of the strain field is of order eight hours. Thus, the number of independent strain events represented by these PDFs is approximately a factor of 160 less than the total number of observations recorded. The issue of statistical stability is not of great import here, however, as the estimates have converged to stable forms.

One sees at large separation (Fig. 9) near-Gaussian PDFs. The deep data have broader histograms than the shallow at similar mean vertical separation. As mean separation is decreased (Figs. 10, 11), the distributions become progressively more skewed. Also, the difference between the upper and lower depth ranges decreases. Indeed, the 2 m strain shows no significant variation with depth.

In the algorithm used to calculate isopycnal position, density inversions are removed. There is no possibility of observing "crossed isopycnals" in this dataset. The distributions are truncated at $\gamma = 0$. Also, the occurrence of closely spaced isopycnals implies the existence of large density gradients. The finite resolution of the CTD significantly smooths the high gradient regions, artificially separating the isopycnals. As a consequence,

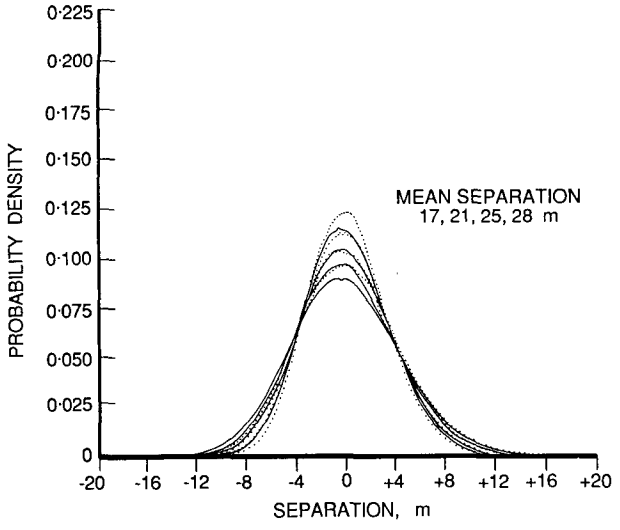

FIG. 9. Probability density of isopycnal separation fluctuation, $\Delta z - \overline{\Delta z}$ from PATCHEX. Data from 100–300 m are drawn with a dotted line, 300–500 m with a solid line. The PDFs become increasingly broad (more variance) with increasing mean separation Δz. The PDFs from the shallow region have less variance than their deep counterparts, at fixed mean separation. The histograms are each based on 1.8×10^6 points.

a precutoff increase in probability is often seen just preceding the truncation. Instrument resolution has little effect on other aspects of histogram form.

It is reasonable to exploit the 2-D view obtained by the CTD to calculate joint depth–time statistics of the strain field. A traditional investigation would be based on the autocorrelation of isopycnals, as a function of depth and time lags. However, the extreme skewness of the separation probability density cautions that the time evolution of the "sheets" might be far different than that of the "layers." This aspect of the field would not be represented by an autocorrelation function.

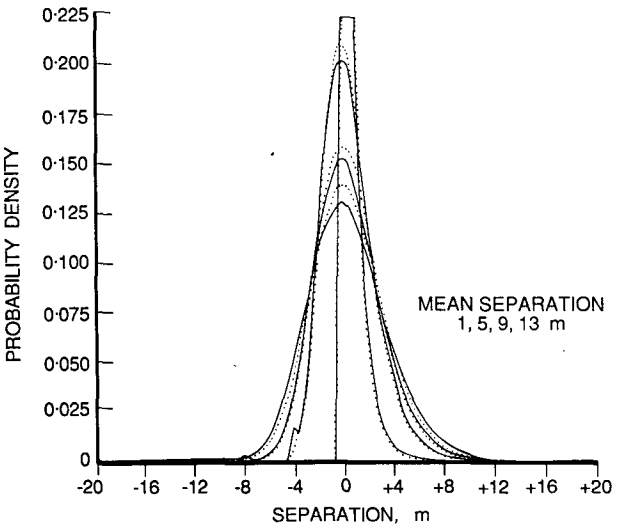

FIG. 10. Probability of $\Delta z - \overline{\Delta z}$, as in Fig. 9, except for smaller separations. The PDF of 1 m separation has been truncated.

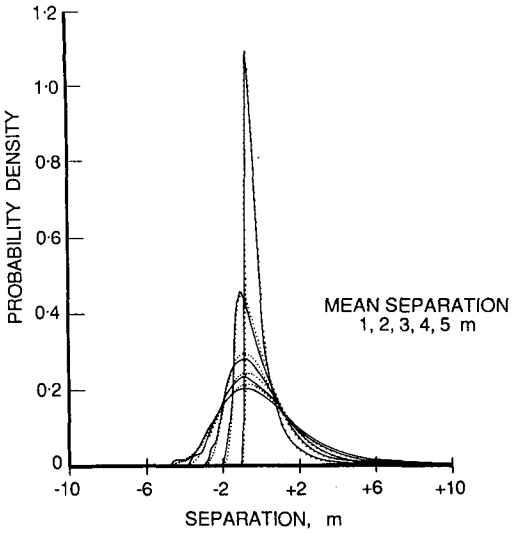

FIG. 11. Probability of $\Delta z - \overline{\Delta z}$, as in Figs. 9 and 10, for very small mean separations. Note the change in vertical scale relative to the previous figures. The histograms representing the upper and lower depth ranges become more nearly identical as the mean separation is decreased.

Here we adopt a rather primitive approach, defining a strain "event" to occur whenever isopycnalseparations exceed twice ($\gamma > 2$:layers) or fall below half($\gamma < 0.5$:sheets) the mean separation. The probability of occurrence of sheet and layer events is given by the area under the tails of the separation PDFs presented in Figs. 9–11. Events are tracked in both time and density (depth), as separate studies. In the former case, the duration of each event, as well as the average and maximum values of strain are tabulated, at fixed density. This is done for each of the 400 isopycnal pairs followed between depths of 100 and 500 m. An "event" is deemed to start when the separation associated with a given isopycnal pair first exceeds the threshold. The event ends when γ returns to values $0.5 < \gamma < 2$. The mean separation between isopycnals is 2 m. A 24 minute time-average is employed prior to searching for the events. This reduces the influence of the isolated regions of irregularity seen in Fig. 6.

Histograms of event occurrence as a function of event duration and extreme/average strain during the event are presented in Fig. 12. The histograms are normalized such that the sum of the layer and sheet events is unity. The relative height of the distributions for sheets and for layers thus gives an index of relative likelihood of occurrences.

As expected, many more "sheet" events occur than "layer" events. The typical sheet also lasts longer than typical layer, although the relationship between maximum strain and event duration is similar for both. Longer lived events are more likely to achieve more extreme values of strain than shorter lived events.

When one compares event duration with average strain rather than extreme, a different pattern emerges. The average strain of events which last longer than

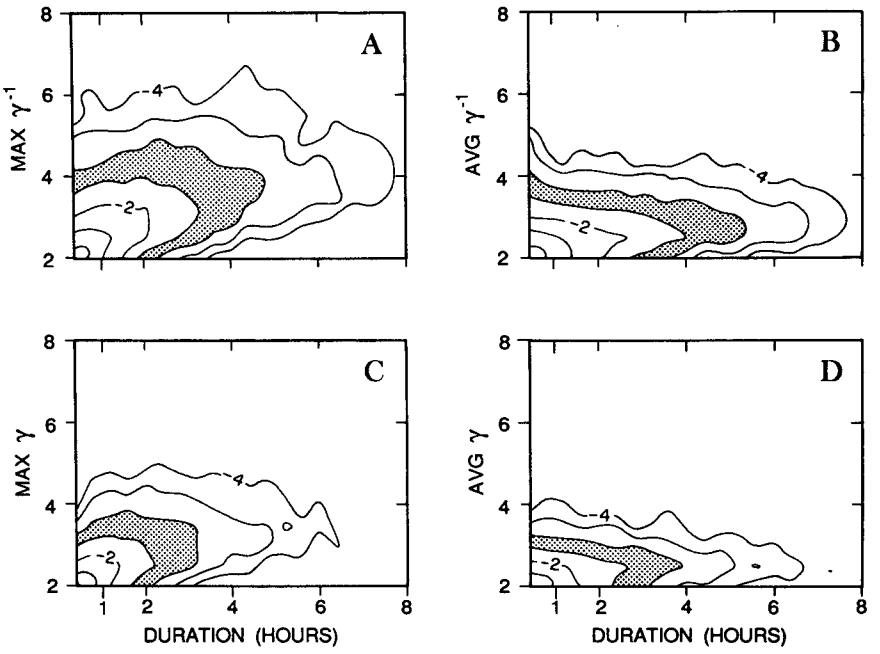

FIG. 12. Contour maps of the relative probability of occurrence of strain events, for $\bar{\Delta}z = 2$ m. Maps are normalized such that the volume under maps A and C sums to unity; similarly for B and D. Probability is contoured logarithmically, with intervals separated by 5 db. The interval between −2.5 and −3 (−25 to −30 db) is shaded. The ordinate indicates the degree of distortion observed, with isopycnals being encountered two through eight times closer together than average (sheets; A, B) or two through eight times farther apart (layers; C, D). The longer a strain event exists, the greater the extreme value strain. The average value of strain is independent of event duration, for those events which last longer than two hours.

about 2 hours is typically the same. Long lived layers are typically six meters thick ($\Delta z/\overline{\Delta z} = 3$). Long lived sheets are most often found to be ⅔ m thick. This result is most likely influenced by the finite resolution of the CTD.

A similar study can be made of the extent of these extreme strain events in density space. When two isopycnals are brought close together (or far apart) by the motion field, what is the likelihood that the adjacent pair will also be close together/far apart? To address this issue, a series of 2016 15-minute average vertical profiles of the strain are formed. Isopycnal pairs of 2 m mean separation are considered. Again, strain "events" are defined, with $\gamma > 2$ or $\gamma < 0.5$ giving the threshold of occurrence of "layers" and "sheets," respectively. Stepping through each profile with increasing depth (density) the number of isopycnals participating in each event, as well as the extreme and depth averaged value of strain in the event are tabulated. Histograms are presented in Fig. 13.

When extreme layers are seen ($\gamma > 3$) only one or two isopycnal pairs participate. On rare occasion, when five isopycnal pairs are involved in a "layer," the maximum strain experienced by any of them is just over the threshold. This corresponds to a 6 m region of the ocean swelling to a thickness of 12 m. No matter what the maximum thickness, it is always most likely to find one or two isopycnal pairs participating in a layer.

The situation for sheets is far different. Here the histogram has a clearly defined ridge. As the maximum value of γ^{-1} increases, the number of isopycnals most likely to be involved also increases.

As with the event duration study, a greater number of sheets is seen than layers. This is an inherent consequence of working in isopycnal following coordinates. In some sense, it takes more isopycnals to form a sheet than a layer.

In terms of overall statistics, the depth and duration studies give a slightly different view of the strain field. Events occur 8.86 percent of the time in the depth study. Sheet events are seen 6.25 percent of the time, while layer events occur with a frequency of 2.61 percent. For the duration study, events are seen 7.14 percent of the time. Sheets occur with 5.26 percent frequency and layers with 1.88 percent frequency. These quantitative statistical results are a strong function of both the mean separation between isopycnals, $\overline{\Delta z}$ and the choice of event threshold, ($\gamma > 2$, $\gamma < 0.5$). This can be seen from direct examination of the separation PDFs in Fig. 11. Selecting a different $\overline{\Delta z}$ corresponds to changing the PDF being considered. Altering the threshold values of γ changes the region of the high and low γ tails of the PDF which are defined as "events."

The difference in depth and duration statistics is related to the nature of the statistical test. For example,

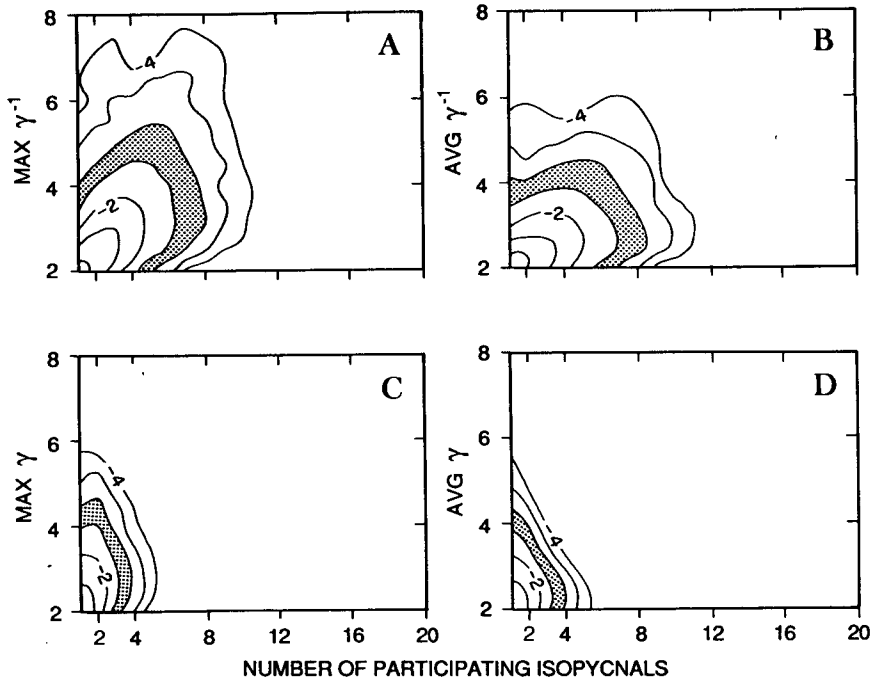

FIG. 13. As in Fig. 12, except here the number of adjacent isopycnals participating in an event is tracked. It is common for many adjacent isopycnals to participate in a sheet. Layers are usually associated with a single isopycnal pair.

consider a single isopycnal pair which comes together to form a "sheet event" for one hour. The duration study would count this as a single event, lasting one hour. The depth (density) study would count this as four events (one occurrence in each of the four 15-minute average profiles), each involving a single isopycnal pair. Also, under the ground rules of the event duration study, an event can "end" by propagating vertically from one isopycnal surface to the next. The visual lifetime of the events seen in Figs. 5–7 is greater than the statistical lifetime defined in this study.

5. Discussion

a. Reversible fine structure

We have somewhat arbitrarily adopted the position that all of the observed fine structure is reversible, being created through the distortion of a smooth "underlying" density field by a perhaps Gaussian velocity field. By tracking isopycnals, rather than isothermal or isohaline surfaces, it is hoped to minimize the influence of large scale intrusive features on the observations. Yet there are no grounds to deny the existence of intrusions.

The following sections explore some of the consequences of the reversible fine structure interpretation. For the purpose of discussion, the observed "sheets and layers" are taken to be the result of local constructive interference in the orbital displacement of the internal wavefield. The features can propagate across isopycnal surfaces, although their persistence time–distance (as with any constructive interference) is typically smaller than the characteristic times–lengths of the constituent motions which interfere. Layers disappear as a result of lateral divergence of the underlying current field. This divergence need not be opposed by frictional effects, as discussed by Stommel and Federov (1967) and others. To the extent that the fine structure is truly reversible, there is no implication of dissipative processes.

In dealing with a significantly skewed scalar field, the techniques traditionally used to track the state of the field (here, isopycnal following) require re-examination. For example, one passes through more isosurfaces per unit distance in high gradient regions than in low, by definition. Averages taken along isopycnal surfaces will be biased toward the high gradient regions, to an extent determined by the skewness of the PDF of separation. In terms of the simple sheet and layer point of view, the waters of the sea are found in the layers, while the isopycnal surfaces congregate in the sheets.

Consistent with this viewpoint, data obtained from along isopycnal tows (space-series) can also be expected to have skewed distributions of vertical isopycnal separation, at the fine scale. Isopycnal separation data obtained from Lagrangian floats should be more nearly Gaussian. As isopycnals congregate to form high gradient sheets, the floats will be exhausted laterally. Only

the isopycnals converge in high gradient regions. The water does not, being incompressible.

b. The non-Gaussianity of strain

Histograms of strain (Figs. 9–11) become increasingly skewed with decreasing mean separation. This reflects the fact that isopycnals which are closer together than their mean separation tend to remain close together for a relatively long time, as they experience the same motion field. Isopycnals which are farther apart than their mean separation experience a greater difference in advecting velocity. The relative separation between such isopycnals can be expected to change more rapidly. The sampling format of this experiment, with profiles spaced at equal increments of time, necessarily results in skewed isopycnal separation PDFs.

At very small separations, it is conjectured that the PDFs approach log-normal form. Consider the vertical advection of nearby isopycnals in a Gaussian vertical velocity field.

$$\partial z(t, \rho_1)/\partial t \equiv w(z(t, \rho_1))$$
$$\partial z(t, \rho_2)/\partial t \equiv w(z(t, \rho_2)). \quad (6)$$

Here $z(t, \rho_i)$ is the depth at which density ρ_i is encountered at time t. Isopycnal separation is conveniently described by expanding the vertical velocity field as a Taylor series about the mean depth of the isopycnal pair, $\bar{z}$. Differencing the above equations then leads to:

$$\frac{\partial(\Delta z)}{\partial t} = \left.\frac{\partial w}{\partial z}\right|_{z=\bar{z}} \Delta z + \cdots \quad (7)$$

$$\frac{\partial(\log(\Delta z/\overline{\Delta z}))}{\partial t} \approx \left.\frac{\partial w}{\partial z}\right|_{z=\bar{z}}. \quad (8)$$

Here Δz is the instantaneous separation and $\overline{\Delta z}$ is the mean separation for the isopycnal pair. If the rate of strain component $\partial w/\partial z$ has Gaussian statistics, the time derivative of log separation will be Gaussian as well. Integrating with respect to time, it is seen that isopycnal separation will be log-normal provided the vertical gradient, $\partial\hat{\eta}/\partial z$, of the vertical "progressive displacement"

$$\hat{\eta} = \int_0^t w dt' \quad (9)$$

has Gaussian statistics. (Note that the observed displacement field is also influenced by lateral advection).

The relationship between isopycnal separation and the underlying vertical velocity field is given by

$$\Delta z(t)/\overline{\Delta z} = C_0 e^{\partial\hat{\eta}(\bar{z},t)/\partial z}. \quad (10)$$

In order that the expected value $\langle \Delta z(t) \rangle = \overline{\Delta z}$, the constant of integration C_0 is identified as

$$C_0 = \Delta\hat{z}/\overline{\Delta z}, \quad (11)$$

where

$$\Delta\hat{z} \equiv \overline{\Delta z}\langle e^{\partial\hat{\eta}/\partial z}\rangle^{-1} \quad (12)$$

is the median isopycnal separation.

In the log-normal limit, the strain $\hat{\gamma} = \Delta z(t)/\overline{\Delta z} - 1$ is independent of the vertical scale, $\overline{\Delta z}$, over which it is calculated. Strain measurements over a continuum of separations centered at some $\bar{z}$ will be identical. Thus, the log-normal regime is only found at scales shorter than the shortest energetic scale in the strain rate field. In a companion study, it is suggested that log-normal conditions will prevail at vertical scales shorter than about 80 cm, in the absence of overturning. Given the finite spatial resolution of the CTDs used in this study, it is accurate to state that we have been observing the tendency toward log-normal behavior at small separation, rather than the log-normal field itself.

The attempt to demonstrate the self-similar aspect of the strain field is influenced by the resolution of the CTD, as well as the absence of log-normal conditions at 2–5 m vertical scale. However, the appearance of self-similarity is enhanced by the k^{-1} slope of the strain vertical wavenumber spectrum (Gregg 1977) in the 1–10 m band. It is easily shown that for a process described by a k^{-1} spectrum, the variance per octave of the field is constant, independent of wavenumber. The qualitative character of this field as observed at different scales will be similar, provided the ratio of instrument bandwidth to center wavenumber remains fixed.

The fine-scale motion field in the thermocline is reminiscent of a passive scalar field strained by small scale turbulence, as discussed by Batchelor (1959). In the turbulent case, at scales smaller than the viscous cutoff, passive scalars experience a rate of strain which is uniform in space yet changing in time. The randomly oriented strain rate typically increases the magnitude of the spatial gradient of the scalar. This tendency to increase scalar variance at small scales is countered by molecular diffusion. In balancing the effects of strain rate and diffusion a characteristic spectral form is established.

The analogy between internal wave straining in the thermocline and the straining of a passive scalar at scales smaller than the viscous cutoff is less than ideal. For "reversible fine structure", there is no interplay between one phenomenon which turns layers into sheets, and a second phenomenon, which destroys the sheets. As adjacent isopycnals "random-walk" away from each other, pressure gradients are established in the fluid which encourage their return. Thus no characteristic balance is implied. It is tempting to hypothesize a Batchelor-like model of "not quite reversible" fine structure, with some dissipative process occurring selectively. Such a modeling effort is beyond the scope of this work.

If we consider the depth dependence of the strain field, indexing successive isopycnal pairs by their mean

depth, $\bar{z}$, mean separation, and time, we see

$$\gamma(t, \bar{z}, \overline{\Delta z}) = C_0 e^{\partial\hat{\eta}(\bar{z},t)/\partial z} \approx \frac{\Delta\hat{z}}{\overline{\Delta z}}\left[1 + \frac{\partial\hat{\eta}}{\partial z}(\bar{z}, t) + \frac{1}{2}\left(\frac{\partial\hat{\eta}}{\partial z}(\bar{z}, t)\right)^2 + \cdots\right]. \quad (13)$$

A vertical wavenumber spectrum of strain will have variance at the same scales as $\partial\hat{\eta}/\partial z$, as well as much smaller scales, due to the higher order terms in the approximation. This point was emphasized by Desaubies and Gregg (1981). Frequency spreading will also occur, resulting in the creation of the subinertial variance seen in Fig. 4. Note that the form of the semi-Lagrangian vertical wavenumber spectrum depends not only on the form of the Eulerian spectrum but also on its magnitude. The more energetic the motion field, the greater the observed spread of variance to space-time scales beyond those in the Eulerian strain field. In contrast to the commonly discussed problem of "fine structure contamination" of Eulerian oceanographic measurements (Phillips 1971; McKean 1974), here it is the isopycnal following view of the world which is becoming "distorted" by a Gaussian velocity field.

c. *Property gradients*

The non-Gaussianity of the strain field can be a consequence of the "passive" advection of isopycnals by a Gaussian velocity field. Is this phenomenon of any importance to ocean dynamics?

In the stratified regions of the ocean it is usually the case that properties vary more rapidly in the cross-isopycnal direction than in an isopycnal plane. If one describes the instantaneous vertical gradient of such a property, θ, in density coordinates,

$$\frac{\partial\theta}{\partial z}(t, \bar{z}, \overline{\Delta z}) = \frac{\theta(\rho_1) - \theta(\rho_2)}{\Delta z(t, \bar{z}, \overline{\Delta z})} = \frac{\theta(\rho_1) - \theta(\rho_2)}{\overline{\Delta z}} \frac{\overline{\Delta z}}{\Delta z(t, \bar{z}, \overline{\Delta z})}. \quad (14)$$

The instantaneous value of the gradient is the product of the mean gradient and the normalized inverse separation, γ^{-1}. The inverse strain modulates vertical gradients of properties in the sea. It follows that fluctuations of the vertical gradients of a variety of passive quantities such as temperature or density itself, will have identical probability distributions in isopycnal following coordinates, at fine scale. Knowledge of the PDF of γ (and hence, γ^{-1}) allows one to predict fluctuation statistics without the need to linearize about small values of the strain.

While gradient fluctuations may appear as a "subgrid scale" effect to large scale modelers, not all aspects of the gradient modulation problems disappear with spatial averaging. In particular, since the vertical gradients of many quantities are modulated by the identical strain field, averages of the products of gradients can be expected to differ significantly from products of the averages.

d. *Zooplankton and strain*

From acoustic scattering studies zooplankton are known to congregate in regions of high density gradient. The scattering layers appear to track the vertical displacements of the internal wavefield. Is the zooplanktonic world inherently skewed?

To the extent that the plankton are ideal Lagrangian drifters, the population can be treated as a passive scalar field. If a particular plankton population exists between densities ρ_1 and ρ_2, the concentration of plankton will not be affected by reversible fine-structure. As isopycnals come together to form sheets, the plankton will be exhausted laterally, along with the water. In particular, acoustic scattering strength should be unaffected, as this depends primarily on the number of organisms per unit volume. What of the observations to the contrary? Possible explanations include:

- To an acoustician, the distinction between a scattering "layer" and a scattering "sheet" is a second order effect. If there are a lot more "targets" between densities ρ_1 and ρ_2 than at neighboring densities, the plankton are a useful tracer of motion. This usefulness is enhanced by the fact that at any given time, over most of the internal acreage of the sea, isopycnals ρ_1 and ρ_2 are closer together than average. Hence, most acoustic observations will see a clearly defined scattering zone.
- The compressibility of the plankton may be slightly different than that of water. As large scale internal waves vertically advect the entire fine scale field, plankton in the layers will find themselves collected against the vertical boundaries of a layer, i.e. the adjacent sheets. This represents a modest cross isopycnal migration by the plankton, with no work being done on their part. It also constitutes a mechanism for actually increasing the concentration of the plankton, resulting in increased acoustic scattering.

e. *Richardson number*

It is instructive to consider an extreme idealization of the reversible fine structure concept. Consider horizontal (isopycnal) flows associated with internal waves. Most of the variance is due to near inertial motion, which changes significantly in time over a fraction of an inertial period. The shear will depend on the depth (density)–time evolution of both the velocity and strain fields.

$$\frac{\partial u}{\partial z}(t, \bar{z}, \overline{\Delta z}) = \frac{u(\rho_1, t) - u(\rho_2, t)}{z(\rho_1, t) - z(\rho_2, t)} = \frac{\Delta u(t, \bar{z}, \overline{\Delta z})}{\overline{\Delta z}} \gamma^{-1}(t, \bar{z}, \overline{\Delta z}) \equiv \frac{\Delta u(t, \bar{z}, \overline{\Delta z})}{\overline{\Delta z}} [N^2(t, \bar{z}, \overline{\Delta z})/\overline{N^2}(\bar{z}, \overline{\Delta z})]. \quad (15)$$

A Fourier description of the shear will involve a convolution of the Fourier frequency coefficients of the "unstrained" quasi-linear shear and those of the "inverse strain", γ^{-1}.

In the extreme limit of a time independent velocity field, $u(\rho, t) = u(\rho)$, the Richardson number is given by

$$\mathrm{Ri}(t, \bar{z}, \overline{\Delta z}) = N^2(t, \bar{z}, \overline{\Delta z})/(\partial u/\partial z)^2 = \overline{N^2}/(\Delta u/\overline{\Delta z})^2 \cdot \gamma = \overline{\mathrm{Ri}} \cdot \gamma. \quad (16)$$

When isopycnals are twice as close together as average, the squared Väisälä frequency is increased by a factor of two. Squared shear is increased by a factor of four. Local shear instability will thus be associated with sheets rather than layers, in this idealized model.

One can reconcile the observation that the "internal wave scale" Richardson number is of order 1 (Munk 1981) with the concept of fine scale instability by invoking this reversible fine structure model. Strain sufficient to reduce the Richardson number from 1 to ¼ occurs approximately 0.1% of the time in PATCHEX. (But was the Richardson number unity before the strain started to act?)

A true devil's advocate might make the following argument: "Most of the shear in the thermocline is associated with near inertial motion. The shear direction rotates at the inertial frequency. However, shear magnitude, of relevance to the Richardson number, varies only over much longer time scales, with the passage of near inertial groups (Pinkel 1983). Thus, time fluctuations in Richardson number depend almost entirely on variations in strain . . ."

The above viewpoint contrasts radically with that advanced in the various Garrett–Munk internal wave models. In these models, internal wave shear variation provides the total variability in Richardson number. The Väisälä frequency is considered a climatological constant. Desaubies and Smith (1982) account for variations in both shear and strain in their simulation of Richardson number statistics. However, they assume that strain and shear are statistically independent, Gaussian quantities.

One can add a hint of dynamics to the above discussion by noting that, as water is ejected laterally from between isopycnal surfaces, vortex lines in the direction of the horizontal strain will be stretched, resulting in an increased horizontal shear normal to the strain direction. Vortex lines oriented at right angles to the lateral strain will be unaffected. Progress toward a realistic model of internal wave breaking awaits accurate observations of the strain-shear correlation. Attacking this problem in density coordinates should prove fruitful.

f. Potential vorticity conservation and relative vorticity

In the absence of dissipation, Ertel potential vorticity is conserved. Following a fluid parcel that is bounded in the vertical by densities ρ_1 and ρ_2, the quantity $(\zeta + f)/\Delta z$ is constant. Here ζ is the component of relative vorticity normal to the isopycnal surface, f is the Coriolis frequency, and Δz is the separation between isopycnals. If ζ_0 is the relative vorticity of a parcel when $\Delta z = \overline{\Delta z}$, the change in instantaneous relative vorticity is given by

$$\frac{\Delta\zeta}{\zeta_0 + f} = \frac{\Delta z}{\overline{\Delta z}} - 1 \equiv \hat{\gamma}. \quad (17)$$

Since $\hat{\gamma}$ is highly skewed, is ζ also?

From the perspective of a fluid parcel which is free to move laterally (rather than the "tunnel vision" view obtained by following isopycnals in depth, $\hat{\gamma}$ might not be as highly skewed. Strain is more nearly Gaussian in the Lagrangian frame, and relative vorticity as well.

Significant fluctuations in relative vorticity are required in order that potential vorticity be conserved. At large vertical scale, these fluctuations are presumably provided by the wavefield itself. At smaller scale, beyond the energetic scales in the Eulerian strain field, the nature of the dynamics is unclear. To adjust to a relative vorticity change comparable to f over a horizontal scale L, velocity fluctuations of order Lf are required. For L = 1 km, the associated perturbation velocity is approximately 1.2 cm s^{-1}, at 30° latitude. This is smaller than typical oceanic wavefield velocities, although comparable to velocity *changes* over a 1 km horizontal scale.

Note the apparent inconsistency in viewpoint between the present discussion and that of the Richardson number. Here we suggest that the horizontal velocity field responds to the strain field, in order to conserve both mass and potential vorticity. Above, the time variation of the horizontal velocity field was assumed to be independent of strain.

Acknowledgments. The authors would like to thank R. E. Davis, F. Henyey, G. Holloway, and P. Muller for useful discussions. E. Slater, L. Green and M. Goldin designed and operated the CTD profiling system used to collect these data. This program was sponsored by the office of Naval Research under Contract N00014-90-J-1099 and the National Science Foundation under OCE 87-11936.

APPENDIX

In this work, a finite difference approximation is used to describe the strain field in a isopycnal following reference frame. The relation between a finite difference and a derivative is well known. It is reviewed here for the sake of completeness.

If the isopycnal vertical displacement field, $\eta(t, \bar{z})$, is described over the depth interval $(0, H)$ by a Fourier series,

$$\eta(t, \bar{z}) = \sum_k A(t, k) e^{ik\bar{z}}$$

then the associated strain field is given by

$$\frac{\partial \eta}{\partial \bar{z}} = i \sum_k kAe^{ik\bar{z}}.$$

The strain variance, for a stationary, homogeneous process, is

$$\left\langle \left(\frac{\partial \eta}{\partial z} \right)^2 \right\rangle = \sum_k k^2 \langle AA^* \rangle$$
$$= \sum_k k^2 S(k) \Delta k$$
$$= \sum_k \Gamma(k) \Delta k.$$

Here, the brackets refer to either ensemble or time averaging, $S(k)$ is the power spectral estimate of displacement, $\Gamma(k)$ is the power spectral estimate of strain and $\Delta k = 2\pi/H$ is the resolution bandwidth of the spectral estimates.

The isopycnal depth-difference time series, discussed in the text, is related to

$$\Delta\eta(t, \bar{z}, \overline{\Delta z}) = \eta(t, Z(\rho_1)) - \eta(t, Z(\rho_2))$$
$$= \sum_k A(t, k)(e^{ikZ_1} - e^{ikZ_2})$$
$$= 2 \sum_k Ae^{ik\bar{z}} \sin \frac{k\overline{\Delta z}}{2}$$

where $\bar{z} = (Z(\rho_1) + Z(\rho_2))/2$ and $\overline{\Delta z} = Z(\rho_1) - Z(\rho_2)$. The depth-difference variance is

$$\langle \Delta\eta^2 \rangle = 4 \sum_k \langle AA^* \rangle \sin^2 \frac{k\overline{\Delta z}}{2}$$
$$= \overline{\Delta z}^2 \sum_k \Gamma(k) \operatorname{sinc}^2 \frac{k\overline{\Delta z}}{2\pi} \Delta k$$

where $\operatorname{sinc}(x) = \sin(\pi x)/(\pi x)$. The sinc^2 function has unit value when $k\overline{\Delta z}$ is small relative to π. It falls to a local zero when $k\overline{\Delta z} = 2\pi$. The sinc^2 thus serves to low-pass filter the strain spectrum. If the strain spectrum is band limited, i.e., $\Gamma(k) = 0$ for $k > k_0$, then one can always determine a differencing interval $\overline{\Delta z_0} \ll 2\pi/k_0$ such that the finite difference strain is a good approximation to the total strain field. In general, as one reduces the differencing interval $\overline{\Delta z}$, the filter broadens and less of the spectral variance is filtered out. If the strain spectrum is independent of wavenumber, the observed strain variance will vary like $\overline{\Delta z}^{-1}$ as the differencing interval is altered. The isopycnal depth-difference variance, $\langle \Delta\eta^2 \rangle = \langle (\partial\eta/\partial\bar{z})^2 \rangle \overline{\Delta z}^2$ will thus increase linearly with $\overline{\Delta z}$, as is seen in Fig. 8.

REFERENCES

Batchelor, G. K., 1959: Small scale variation of convected quantities like temperature in a turbulent fluid. Part I: General discussion of the case of small conductivity. *J. Fluid Mech.*, **5**, 113–33.

Desaubies, Y. J. F., and M. C. Gregg, 1981: Reversible and irreversible fine structure. *J. Phys. Oceanogr.*, **11**, 541–556.

——, and W. K. Smith, 1982: Statistics of Richardson number and instability in oceanic internal waves. *J. Phys. Oceanogr.*, **12**, 1245–1259.

Gargett, A. E., P. J. Hendricks, T. B. Sanford, T. R. Osborn and A. J. Williams III, 1981: A composite spectrum of vertical shear in the upper ocean. *J. Oceanogr.*, **11**, 1258–1271.

Garrett, C. J. R., and W. H. Munk, 1971: Internal wave spectra in the presence of fine structure. *J. Phys. Oceanogr.*, **1**, 196–202.

——, and ——, 1972: Space–time scales of internal waves. *Geophys. Fluid Dyn.*, **2**, 225–264.

——, and ——, 1975: Space–time scales of internal waves: A progress report. *J. Geophys. Res.*, **80**, 291–299.

——, and ——, 1979: Internal waves in the ocean. *Ann. Rev. Fluid Mech.*, **11**, 339–369.

Gregg, M. C., 1977: A Comparison of fine structure spectra from the main thermocline. *J. Phys. Oceanogr.*, **7**, 33–40.

——, 1987: Diapycnal mixing in the thermocline: A review. *J. Geophys. Res.*, **92**, 5249–5286.

Holloway, G., 1983: A conjecture relating oceanic internal waves and small-scale processes. *Atmos.-Ocean*, **21**, 107–122.

McKean, R. S., 1974: Interpretation of internal wave measurements in the presence of fine structure. *J. Phys. Oceanogr.*, **4**, 200–213.

Muller, P., 1984: Small scale vortical motions. *Internal Gravity Waves and Small-Scale Turbulence, Proc., Hawaii Winter Workshop*, P. Muller and R. Pujalet, Eds., Hawaii Institute of Geophysics, 249–262.

Munk, W. H., 1981: Internal waves and small scale processes. *Evolution of Physical Oceanography, Scientific Surveys in Honor of Henry Stommel*, B. A. Warren and C. Wunsch, Eds., MIT Press, 623 pp.

Phillips, O. M., 1971: On spectra measured in an undulating layered medium. *J. Phys. Oceanogr.*, **1**, 1–6.

Pinkel, R., 1975: Upper ocean internal wave observations from *FLIP*. *J. Geophys. Res.*, **80**, 3892–3910.

——, 1983: Doppler sonar observations of internal waves: wave-field structure. *J. Phys. Oceanogr.*, **13**, 804–815.

——, 1984: Doppler sonar observations of internal waves: The wavenumber frequency spectrum. *J. Phys. Oceanogr.*, **14**, 1249–1270.

——, A. J. Plueddemann and R. G. Williams, 1987: Internal wave observations from *FLIP* in MILDEX. *J. Phys. Oceanogr.*, **17**, 1737–1757.

Sherman, J. T., 1989: Observations of fine-scale vertical shear and strain in the upper-ocean. Ph.D. thesis, University of California, San Diego,

——, and R. Pinkel, 1991: Estimates of the vertical wavenumber frequency spectra of vertical shear and strain. *J. Phys. Oceanogr.*, in press.

Stommel, H., and K. N. Federov, 1967: Small scale structure in temperature and salinity near Timor and Mindanao. *Tellus*, **19**, 306–325.